Enthalpy–Entropy Correlations in Reactions of Aryl Benzoates with Potassium Aryloxides in Dimethylformamide

IRINA A. KHALFINA, VLADISLAV M. VLASOV

N. N. Vorozhtsov Novosibirsk Institute of Organic Chemistry, the Siberian Branch of Russian Academy of Sciences, Novosibirsk, 630090, the Russian Federation

Received 11 July 2012; revised 10 October 2012; accepted 21 October 2012

DOI 10.1002/kin.20763
Published online 22 February 2013 in Wiley Online Library (wileyonlinelibrary.com).

ABSTRACT: Temperature dependences of the relative reactivity of potassium aryloxides $XC_6H_4O^-K^+$ toward 4-nitrophenyl (**1**), 3-nitrophenyl (**2**), 4-chlorophenyl (**3**), and phenyl (**4**) benzoates in dimethylformamide (DMF) were studied using the competitive reactions technique. The rate constants k_X for the reactions of **1** with potassium 4-cyanophenoxide, **2** with potassium 3-bromophenoxide, **3** with potassium 3-bromo-, 4-bromo-, and unsubstituted phenoxides, **4** with potassium 4-methoxy- and 3-methylphenoxides were measured at 25°C. Correlation analysis of the relative rate constants $k_X/k_{H(3\text{-}Me)}$ and differences in the activation parameters ($\Delta\Delta H^{\neq}$ and $\Delta\Delta S^{\neq}$) of competitive reactions revealed the existence of six isokinetic series. We investigated the substituent effect of X on the activation parameters for each isokinetic series and concluded that the reactions of aryl benzoates $PhCO_2C_6H_4Y$ with potassium aryloxides in DMF proceed via a four-step mechanism. The large $\rho^0(Y)$ and ρ_{XY} values at 25°C obtained for the reactions of **1–3** with potassium aryloxides with an electron-donating substituent refer to the rate-determining formation of the *spiro*-σ-complex. The Hammett plots for the reactions of **1** and **2** exhibit a downward curvature, causing the motion of the transition state for the rate-determining step according to a Hammond effect as the substituent in aryloxide changes from electron-donating to electron-withdrawing. Analysis of data in the terms of two-dimensional reaction coordinate diagrams leads to the conclusion that significant anti-Hammond effects arise in the cases of ortho-substituted and unsubstituted substrates. It was shown that the isokinetic and compensation effects observed for the reactions of aryl benzoates with potassium aryloxides in DMF can be interpreted in the terms of the electrostatic bonding between the reaction centers. © 2013 Wiley Periodicals, Inc. Int J Chem Kinet 45: 266–282, 2013

Correspondence to: V. M. Vlasov; e-mail: vmvlasov@nioch.nsc.ru.

INTRODUCTION

One of the most common and important reactions in organic chemistry is that of aryl esters with nucleophiles. Acyl group transfer reactions have been studied by several groups, and there is now considerable data on the kinetics and mechanisms of those processes [1–49]. Two distinct reaction mechanisms, concerted A_ND_N and stepwise addition-elimination $A_N + D_N$, have been suggested. As a rule, the aminolysis reactions of aryl esters proceed through the addition-elimination mechanism, in which the rate-determining step (RDS) is dependent on the basicity of the entering amine and the leaving group [14,21–27,29–40,42–44]. The evidence provided is a nonlinear Brønsted-type plot that has often been observed for the reactions of esters with a good leaving group [25,26,29,30,32–34]. However, the stepwise mechanism for the reactions of 2,4-dinitrophenyl acetate with secondary alicyclic amines shifts to the concerted process when the solvent is changed from water to ethanol/water mixtures [45]. Moreover, the corresponding reactions of 2,4,6-trinitrophenyl acetate in water proceed via the concerted mechanism [45].

The reactions of carboxylic esters with anionic nucleophiles have not been completely elucidated. Williams and coworkers have concluded that the nucleophilic substitution reactions of 4-nitrophenyl acetate with a series of aryloxides proceed through the concerted mechanism. The evidence consisted mainly of the absence of a break in the Brønsted-type plot when the pK_a value of the incoming aryloxide corresponded to that of the leaving 4-nitrophenoxide [1,5,9,11,13]. The concerted mechanism has been supported by Jenck and colleagues [6], Rossi and coworkers [12,15], and Castro et al. [18–20], as well as the kinetic isotope effect studies of Hengge [4,7,8,17].

On the contrary, Buncel et al. have concluded that the reactions of phenoxide with a series of substituted phenyl acetates proceed through the stepwise mechanism on the basis of the kinetic result that the σ^0 constants exhibit a better Hammett correlation than the σ^- constants [2,3,10,41]. A similar conclusion has been drawn from the kinetic studies of the reactions of aryl benzoates with OH^-, CN^-, and N_3^- ions [16,28,40]. The stepwise mechanism has been supported through the enthalpy–entropy correlations for the reactions of 4-nitro- and 2,4-dinitrophenyl benzoates with substituted phenols in the presence of potassium carbonate [46–48].

In the previous work, we have reported that the reactions of 2,4-dinitrophenyl benzoate (**5**) with a series of aryloxides in dimethylformamide (DMF) proceed through the stepwise mechanism in which the *spiro*-σ-complex is an intermediate. The downward-curved Hammett plot has been understood as a change in the RDS within a given mechanism upon changing the substituent from the electron-donating substituent (EDS) to electron-withdrawing substituent (EWS) [49].

We have now expanded our study to the reactions of 4-nitrophenyl, 3-nitrophenyl, 4-chlorophenyl, and phenyl benzoates (**1**, **2**, **3**, and **4**, respectively) with the series of potassium aryloxides in DMF at four temperatures in the range from −15 to 70°C to obtain more conclusive information about the reaction mechanism (Scheme 1).

EXPERIMENTAL

Materials

Aryl benzoates **1–4** (see Fig. 1) used in the present study were prepared as described [50]. Their purity was checked by means of their melting point and spectral data such as IR and ^{1}H NMR characteristics. Commercial substituted phenols of chemically pure grade were purified by standard methods. Potassium aryloxides were prepared from the reactions of substituted phenols with potassium methoxide in absolute methanol [51]. Commercial DMF of analytical grade was dried over 4 Å molecular sieves and distilled over calcium hydride under reduced pressure.

Procedures

The direct-measurement kinetic method has been used to determine the rate constants k_X for the relative slow reactions of **1** with potassium 4-cyanophenoxide, **2** with potassium 3-bromophenoxide, **3** with potassium 3-bromo-, 4-bromo-, and unsubstituted phenoxides, **4** with potassium 4-methoxy- and 3-methylphenoxides ($t_{1/2} > 4$ s). In a typical procedure, the glass reactor was initially charged with 5 mmol of aryloxide in 50–100 mL of DMF, placed in the circulating constant-temperature bath and heated to 25 ± 0.2°C. The magnetic stirrer was turned on. The solution of 0.5 mmol of aryl benzoate (0.2 mmol for the reactions of **3** with 3-bromo- and 4-bromophenoxides) in 1 mL of DMF was adjusted to the same temperature and added in one portion. From this moment, the reaction was timed. Samples were drawn at prespecified time intervals. Approximately, 10 samples were collected during the course of each reaction. The frequency of sample collection varied and was dictated by the reaction condition. Samples (3–5 mL) were collected in 10-mL test tubes filled with 5 mL of the cooled mixture of diethyl ether and water (2:3). The test tubes were then shaken

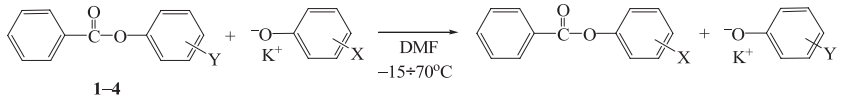

1–4

X = 4-MeO, 4-Me, 3-Me, H, 4-Cl, 4-Br, 3-Br, 3-NO_2, 4-CN

Y = 4-NO_2 (**1**), 3-NO_2 (**2**), 4-Cl (**3**), H (**4**)

Scheme 1

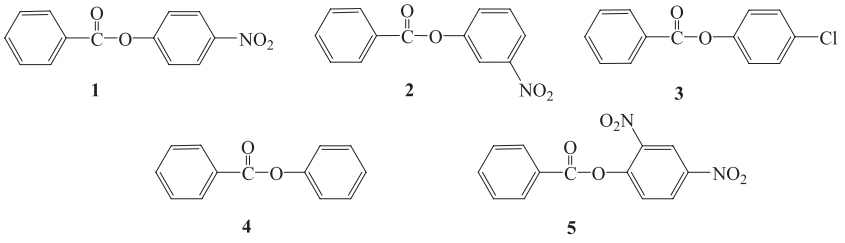

Figure 1 The structures of aryl benzoates (**1–5**) considered in this study.

to stop the reaction. The organic phase was separated; the aqueous phase was extracted with diethyl ether (2 × 3 mL). The extracts were combined with the organic phase, the solvent was distilled off, and the residue was analyzed by gas–liquid chromatography (GLC).

It has previously been shown that the reactions of **1**, **2**, and **3** with potassium 4-cyano-, 3-bromo-, and unsubstituted phenoxides, respectively, are irreversible. The pseudo–first-order rate constants (k_{obs}) were obtained from the linear plots of $\ln(A_\infty - A_t)$ versus t. For the reactions of **4** with 4-methoxy- and 3-methylphenoxides, k_{obs} were obtained from the plots of $\ln(A_\infty - A_t)$ versus t, which were linear up to 90% of the reactions. For the reactions of **3** with 3-bromo- and 4-bromophenoxides, k_{obs} were obtained from the plots of $\ln(A_\infty - A_t)$ versus t, which were linear up to 50% of the reactions. Four different nucleophile concentrations were used to determine the second-order rate constants (k_N) from the slopes of the linear plots of k_{obs} versus potassium aryloxide concentration, which showed near-zero intercepts, indicating that potassium aryloxide does not exist as dimers or other aggregates [52]. The correlation coefficients of the plots were usually higher than 0.999.

It was difficult to use this direct kinetic method for studying fast reactions. As we showed earlier, for the fast reactions of **5** with potassium aryloxides in DMF the relative rate constants k_X/k_H were determined using the competitive reactions technique [49]. In a typical run, the solution of a pair of potassium aryloxides with the pK_a values larger than that of the leaving aryloxide (2.5 mmol + 2.5 mmol) in 50 mL of DMF was placed in the glass reactor equipped with a magnetic stirrer and heated to the desired temperature. The solution of 0.5 mmol of aryl benzoate in 1 mL of DMF was adjusted to the same temperature and then added in one portion. The reaction time was varied from 5 s to 1 h and depended on the substrate reactivity. A sample (3–5 mL) was collected in a 10-mL test tube filled with 5 mL of the cooled mixture of diethyl ether and water (2:3). The test tube was then shaken to stop the reaction. The organic phase was separated; the aqueous phase was extracted with diethyl ether (2 × 3 mL). The extracts were combined with the organic phase, the solvent was distilled off, and the residue was analyzed by GLC. In every case, we found only the resulting aryl benzoates ($PhCO_2C_6H_4X$), which do not practically undergo the reverse reactions. Since for each pair of potassium aryloxides, the competition reactions were performed at equimolar concentrations exceeding the concentration of the substrate by a factor of 5, so the concentration ratio of the products is directly proportional to the ratio of the second-order rate constants for each reaction.

As the reference compound for reactions of **1**−**3** with potassium 4-methoxy-, 3-methyl-, 4-chloro-, and 4-bromophenoxides, we used potassium phenoxides; the relative rate constants k_X/k_H are given in Table I. For potassium 4-methyl-, 3-nitro-, 4-cyano-, and 3-bromophenoxides, we determined the relative rate constants $k_{4\text{-MeO}}/k_{4\text{-Me}}$ (for substrates **1**−**3**), $k_{4\text{-Cl}}/k_{3\text{-NO2}}$ and $k_{3\text{-NO2}}/k_{4\text{-CN}}$ (for substrate **1**), $k_{4\text{-Cl}}/k_{3\text{-Br}}$ (for substrate **2**), which were recalculated to k_X/k_H (Table I). For the reactions of **4** with potassium 4-methoxy- and 4-methylphenoxides, we determined the relative rate constants $k_{4\text{-MeO}}/k_{3\text{-Me}}$ and $k_{4\text{-MeO}}/k_{4\text{-Me}}$, the latter was recalculated to $k_{4\text{-Me}}/k_{3\text{-Me}}$ (Table I).

Table I Relative Rate Constants $k_X/k_{H(3\text{-}Me)}$, Differences in Activation Parameters ($\Delta\Delta H^{\neq}$ and $\Delta\Delta S^{\neq}$) and Selectivity Parameters ($\rho(X)$ and β_{Nuc}) for Competitive Reactions of Aryl Benzoates $PhCO_2C_6H_4Y$ (**I–4**) with Potassium Aryloxides $XC_6H_4O^-K^+$ in DMF

		$k_X/k_{H(3\text{-}Me)}$[a]									
Y	X	−15°C	0°C	25°C	40°C	55°C	70°C	$\Delta\Delta H^{\neq}$ (kJ/mol)[b]	$\Delta\Delta S^{\neq}$ (J/(mol·K))[b,c]	$\rho(X)$[n]	β_{Nuc}[o]
4-NO_2[d]	4-MeO	0.66 ± 0.01	0.63 ± 0.01	0.59 ± 0.03	0.57 ± 0.01			−1.8 ± 0.02	−10.4 ± 0.1	1.40 ± 0.02	−0.31 ± 0.01 (−15°C)
	4-Me[f]	(0.92)	(0.94)	(0.98)	(1.00)			1.0 ± 0.05	3.3 ± 0.2	1.74 ± 0.01	−0.38 ± 0.02 (0°C)
	3-Me	1.26 ± 0.01	1.40 ± 0.06	1.62 ± 0.09	1.76 ± 0.24			4.1 ± 0.03	17.7 ± 0.1	2.19 ± 0.01	−0.49± 0.03 (25°C)
										2.45 ± 0.01	−0.54 ± 0.04 (40°C)
	4-Cl	0.61 ± 0.02	0.38 ± 0.02	0.17 ± 0.03	0.12 ± 0.01			−20.2 ± 0.5	−82.5 ± 1.8	−3.20 ± 0.10	0.70 ± 0.02 (−15°C)
	3-NO_2[g]	(11.5×10^{-3})	(6.5×10^{-3})	(2.7×10^{-3})	(1.7×10^{-3})			−23.4 ± 0.2	−127.8 ± 0.9	−3.29 ± 0.09	0.72 ± 0.01 (0°C)
	4-CN[h]	(16.2×10^{-4})	(8.5×10^{-4})	(3.4×10^{-4})	(2.1×10^{-4})			−24.9 ± 0.05	−150.0 ± 0.2	−3.35 ± 0.09	0.73 ± 0.02 (25°C)
										−3.42 ± 0.11	0.75 ± 0.02 (40°C)
3-NO_2[d]	4-MeO	1.45 ± 0.02	1.46 ± 0.01	1.47 ± 0.01	1.48 ± 0.01			0.2 ± 0.02	4.0 ± 0.07	0.41 ± 0.01	−0.09 ± 0.01 (−15°C)
	4-Me[i]	(1.60)	(1.68)	(1.84)	(1.92)			2.3 ± 0.1	12.7 ± 0.3	0.63 ± 0.01	−0.14 ± 0.01 (0°C)
	3-Me	1.75 ± 0.01	1.95 ± 0.02	2.32 ± 0.02	2.49 ± 0.03			4.4 ± 0.1	21.6 ± 0.4	0.99 ± 0.01	−0.22 ± 0.02 (25°C)
										1.13 ± 0.01	−0.25 ± 0.02 (40°C)
	4-Cl	$8.8 \pm 0.1 \times 10^2$	$5.5 \pm 0.1 \times 10^{-2}$	$2.8 \pm 0.4 \times 10^{-2}$	$2.0 \pm 0.1 \times 10^{-2}$			−18.1 ± 0.1	−90.5 ± 0.4	−3.83 ± 0.03	0.86 ± 0.01 (−15°C)
	4-Br	$6.1 \pm 0.1 \times 10^2$	$3.7 \pm 0.4 \times 10^{-2}$	$1.9 \pm 0.2 \times 10^{-2}$	(1.3×10^{-2})[i]			−18.7 ± 0.2	−95.9 ± 0.8	−4.06 ± 0.05	0.91± 0.01 (0°C)
	3-Br[k]	(1.5×10^{-2})	(8.4×10^{-3})	(4.0×10^{-3})	(2.6×10^{-3})			−21.2 ± 0.6	−117.1 ± 1.3	−4.23 ± 0.01	0.95 ± 0.02 (25°C)
										−4.41 ± 0.05	0.99 ± 0.01 (40°C)

Continued

Table I Continued

4-Cl[d]	4-MeO	1.96 ± 0.11	2.21 ± 0.61	2.34 ± 0.02	2.45 ± 0.01		3.0 ± 0.1	16.8 ± 0.3	−0.94 ± 0.03	0.21 ± 0.01(0°C)
	4-Me[l]	(1.56)	(1.62)	(1.66)	(1.69)		1.1 ± 0.02	7.7 ± 0.06	−1.24 ± 0.06	0.27 ± 0.01(25°C)
	3-Me	1.27 ± 0.01	1.25 ± 0.01	1.24 ± 0.01	1.23 ± 0.02		−0.4 ± 0.01	0.4 ± 0.03	−1.38 ± 0.06	0.31 ± 0.01(40°C)
									−1.50 ± 0.07	0.33 ± 0.01(55°C)
H[e]	4-MeO		2.75 ± 0.02	2.81 ± 0.04	2.87 ± 0.33	2.94 ± 0.02	1.2 ± 0.04	12.6 ± 0.1	−2.20 ± 0.29	0.49 ± 0.03 (25°C)
	4-Me[m]		(1.48)	(1.50)	(1.51)	(1.52)	0.5 ± 0.05	5.0 ± 0.2	−2.25 ± 0.28	0.50 ± 0.03 (40°C)
	3-Me		1	1	1	1	0	0	−2.29 ± 0.29	0.51 ± 0.03 (55°C)
									−2.34± 0.30	0.52± 0.03 (70°C)

[a] Average value determined from at least two parallel runs.
[b] $\Delta\Delta H^{\neq} = \Delta H^{\neq}_{X} - \Delta H^{\neq}_{H}$, $\Delta\Delta S^{\neq} = \Delta S^{\neq}_{X} - \Delta S^{\neq}_{H}$.
[c] At 25°C.
[d] k_X/k_H.
[e] $k_X/k_{3\text{-Me}}$.
[f] $k_{4-Me}/k_H = (k_{4-MeO}/k_H)/(k_{4-MeO}/k_{4-Me})$; $k_{4-MeO}/k_{4-Me} = 0.72 \pm 0.01$ (−15°C), 0.67 ± 0.02 (0°C), 0.60 ± 0.01 (25°C), 0.57 ± 0.03 (40°C).
[g] $k_{3-NO_2}/k_H = (k_{4-Cl}/k_H)/(k_{4-Cl}/k_{3-NO_2})$; $k_{4-Cl}/k_{3-NO_2} = 53.0 \pm 0.5$ (−15°C), 58.5 ± 2.0 (0°C), 63 ± 2.1 (25°C), 71.9 ± 5.3 (40°C).
[h] $k_{4-N}/k_H = (k_{3-NO_2}/k_H)/(k_{3-NO_2}/k_{4-N})$; $k_{3-NO_2}/k_{4-N} = 7.10 \pm 0.3$ (−15°C), 7.65 ± 0.2 (0°C), 7.95 ± 0.1 (25°C), 8.10 ± 0.8 (40°C).
[i] $k_{4\text{-MeO}}/k_{4\text{-Me}} = 0.91 \pm 0.02$ (−15°C), 0.87 ± 0.01 (0°C), 0.80 ± 0.03 (25°C), 0.77 ± 0.03 (40°C).
[j] The relative rate constant k_{4-Br}/k_H at 40°C was calculated from equation $\log(k_{4-Br}/k_H) = -4.98 + 0.97 \times 10^3(1/T)$ r 0.999, s 0.008.
[k] $k_{3-Br}/k_H = (k_{4-Cl}/k_H)/(k_{4-Cl}/k_{3-Br})$; $k_{4-Cl}/k_{3-Br} = 5.85 \pm 0.2$ (−15°C), 6.53 ± 0.1 (0°C), 6.93 ± 0.1 (25°C), 7.73 ± 0.4 (40°C).
[l] $k_{4-Me}/k_H = (k_{4-MeO}/k_H)/(k_{4-MeO}/k_{4-Me})$; $k_{4-MeO}/k_{4-Me} = 1.26 \pm 0.02$ (0°C), 1.37 ± 0.02 (25°C), 1.41 ± 0.10 (40°C), 1.45 ± 0.01 (55°C).
[m] $k_{4-Me}/k_H = (k_{4-MeO}/k_H)/(k_{4-MeO}/k_{4-Me})$; $k_{4-MeO}/k_{4-Me} = 1.86 \pm 0.02$ (25°C), 1.87 ± 0.02 (40°C), 1.90 ± 0.01 (55°C), 1.93 ± 0.01 (70°C).
[n] $\sigma_p^- = -0.27$ (4-MeO), −0.17 (4-Me), 0 (H), 0.19 (4-Cl), 0.23 (4-Br), 1.00 (4-CN); $\sigma_m = -0.07$ (3-Me), 0.39 (3-Br), 0.71 (3-NO_2) [53]; $r \geq 0.992$.
[o] pK_a values of phenols in DMF are correlated with σ^-(X) constants: pK_a(DMF) = –4.6054σ^-(X) + 17.862 [54]; pK_a values of phenols in DMF are calculated: 19.1 (4-$MeOC_6H_4OH$), 18.6 (4-MeC_6H_4OH), 18.2 (3-MeC_6H_4OH), 17.9 (C_6H_5OH), 17.0 (4-ClC_6H_4OH), 16.8 (4-BrC_6H_4OH), 16.1 (3-BrC_6H_4OH), 14.6 (3-$NO_2C_6H_4OH$); 13.3 (4-CNC_6H_4OH); $r \geq 0.990$.

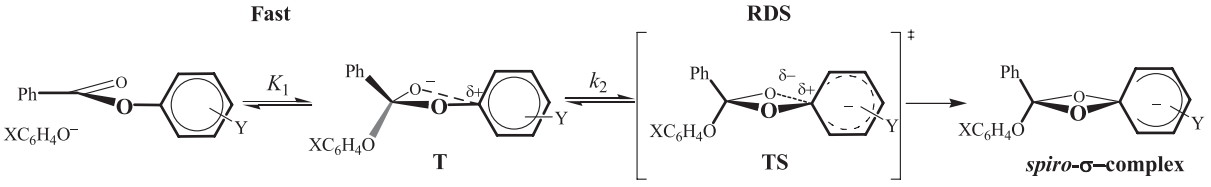

Scheme 2

Analysis

Samples were analyzed by GLC using an LKhM-72 gas chromatograph equipped with a thermal conductivity detector (4000 × 4-mm column packed with 15% of SKTFT-803 on Chromaton-W, carrier gas helium, linear oven temperature programming from 70 to 270°C at the rate of 10 deg/min); the components were quantited by the absolute calibration technique using calibration plots and identified by adding authentic samples.

RESULTS AND DISCUSSION

Effect of Entering Group Substituent on Reaction Selectivity

To investigate the effect of the entering group substituent X on the reaction selectivity, we have used the relative rate constants $k_X/k_{H(3\text{-}Me)}$. As shown in Table I, the relative reactivity of potassium aryloxides toward **1** decreases as the substituent X in the entering group changes from 3-Me to stronger EDS or EWS. A similar effect of the substituent X on the relative reactivity of potassium aryloxides has been found for the reactions of **2**. On the other hand, the k_X/k_H and $k_X/k_{3\text{-}Me}$ values for the reactions of **3** and **4**, respectively, decrease as the electron-donating ability of substituent X decreases. Within the corresponding temperature range, the relative rate constant $k_X/k_{H(3\text{-}Me)}$ changes no more than 8 times for every substrate.

Good linear correlations ($r \geq 0.992$) have been obtained in the plots $\log(k_X/k_{H(3\text{-}Me)})$ versus $\sigma^-(X)$ using potassium aryloxides with an EDS (or an EWS). The selectivity parameter $\rho(X)$ values summarized in Table I were calculated from the Hammett-type equation,

$$\log(k_X/k_{H(3-Me)}) = \rho(X)\sigma^-(X) + \text{const.}$$

The positive $\rho(X)$ values for the reactions of **1** and **2** with potassium aryloxides with an EDS indicate that the k_X value increases with decreasing the electron-donating ability of the substituent X. A similar effect of the entering group substituent has been found for the reactions of **1** with acetophenone oximates in absolute ethanol [55]. As shown in Table I, the $\rho(X)$ value dramatically decreases as the substituent X changes from EDS to EWS. For example, the $\rho(X)$ value decreases from 2.19 to –3.35 at 25°C for the reactions of **1** and from 0.99 to –4.23 at 25°C for the reactions of **2**. Such a large change in the selectivity parameter has been interpreted as a change in the RDS [2,25–28,41]. In addition, for the reactions of **1**, **2** with potassium aryloxides with an EDS, the reactivity–selectivity principle (RSP) fails, since the more reactive system exhibits the larger selectivity [56].

Um et al. have reported that the reactions of **1** with a series of aryloxides in absolute ethanol at 25°C proceed through the stepwise mechanism in which the formation of the symmetric tetrahedral intermediate is the RDS [55,57]. A good Hammett correlation has been obtained with $\rho(X) = -1.96$ [55]. It is evident that the downward-curved Hammett plots obtained for the reactions of **1** and **2** with potassium aryloxides in DMF are contrary to the proposed mechanism.

The reactions of **5** with potassium aryloxides in DMF proceed through the stepwise mechanism in which the *spiro*-σ-complex is an intermediate (Scheme 2). The $\rho(X)$ value has been found to decrease from 0.49 to −3.33 at 25°C as the substituent X changes from EDS to EWS [49]. The similar downward-curved Hammett plots obtained for the reactions of **1** and **2** with potassium aryloxides can be taken as an indirect evidence for the same mechanism.

For the reactions of **3** and **4** with potassium aryloxides with an EDS, the $\rho(X)$ values are negative (Table I). Since the $\rho(X)$ value decreases from –1.24 to –2.20 at 25°C as the leaving group substituent Y changes from 4-Cl to H, one may conclude that the more reactive system exhibits the less selectivity, i.e., the RSP holds. Thus, these reactions can proceed through the formation of a symmetric tetrahedral intermediate [58].

Nevertheless, a failure of the RSP is the characteristic feature for the reactions of aryl benzoates **1–4** with potassium aryloxides in DMF, since for all the reaction series the selectivity increases with increasing temperature (Table I).

Similar conclusions have been drawn on the basis of analysis of the Brønsted-type plots (Table I). It is evident that data obtained for the reactions of **1–4** with potassium aryloxides cannot give any significant information regarding the reaction mechanism.

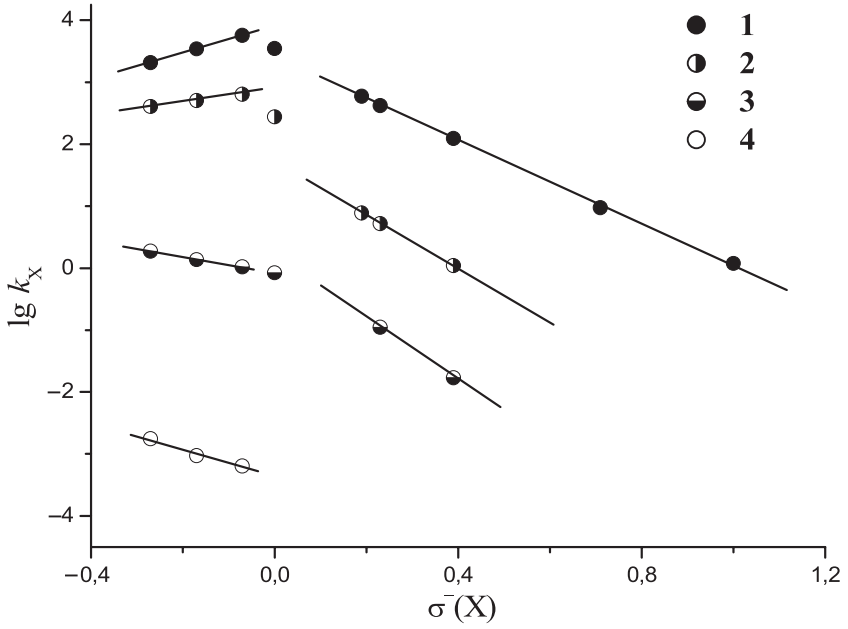

Figure 2 Hammett plots for the reactions of 4-nitrophenyl, 3-nitrophenyl, 4-chlorophenyl, and phenyl benzoates (**1–4**) with potassium aryloxides $XC_6H_4O^-K^+$ in DMF at 25°C.

Using the relative rate constants $k_X/k_{H(3\text{-}Me)}$ at 25°C obtained by the competition kinetic method and the rate constants k_X obtained by the direct-measurement kinetic method for the seven slow reactions at 25°C, the rate constants k_X for other reactions can be calculated. The rate constants k_X determined in this way are summarized in Table II. The Hammett plots for the reactions of **1–4** with potassium aryloxides in DMF at 25°C are shown in Fig. 2.

Effect of Leaving Group Substituent on Reactivity

As shown in Table II, for the reactions of **1–3** with potassium 4-methoxy-, 4-methyl-, and 3-methylphenoxides, the Hammett plots for variations of the substituent Y in the leaving group exhibit much better linear correlations with the σ^0(Y) constants than with the σ^-(Y).

The correlation of reaction rates with the σ^0(Y) constants implies that direct resonance interactions of the leaving group substituent Y and the reaction center do not occur [3]. A similar σ^0 dependence has been observed for many reactions, e.g., for the reactions of aryl benzoates with potassium ethoxide in absolute ethanol [2,3,10,41]. Haake et al. have suggested that in the ground state π interaction of the alcohol oxygen with the carbonyl oxygen results in a partial positive charge on the alcoholic oxygen. So, the large values of ρ^0(Y) indicate a large charge change on the phenolic oxygen on going from ground state to transition state [59].

The ρ^0(Y) values for the reactions **1–3** with potassium aryloxides with an EDS calculated from the Hammett-type equation,

$$\log k_X = \rho^0(Y)\sigma^0(Y) + \text{const},$$

are unusually large and range from 5.47 to 6.66 at 25°C. As shown in Table II, a stronger EDS in aryloxide, $\Delta\sigma^-(X) < 0$, leads to decrease in the ρ^0(Y) value, $\Delta\rho^0(Y)<0$, and the RSP holds. However, a weaker EWS in the leaving group, $\Delta\sigma^0(Y)<0$, leads to decrease and change of the sign of $\rho(X)$, $\Delta\rho(X) < 0$. Good linear correlations ($r \geq 0.989$) have been obtained in the plots $\rho^0(Y)$ versus $\sigma^-(X)$ and $\rho(X)$ versus $\sigma^0(Y)$ for the reactions of **1–3** with aryloxides with an EDS, the cross-interaction constant ρ_{XY} is positive and unusually large, 5.92 at 25°C.

It should be noted that the standard error of ρ_{XY} strongly decreases when the plot changes from $\rho(X)$ versus $\sigma^0(Y)$ to $\rho^0(Y)$ versus $\sigma^-(X)$ (Table II). Since the $\rho(X)$ values are associated with the low standard errors, so the relatively low accuracy of the determined ρ_{XY} value indicates that for the reactions of **1–3** with aryloxides with an EDS use the common scale of the σ_p^0 and σ_m constants of the substituent Y is not sufficiently correct. This problem can also be the cause of

Table II Rate Constants k_X for Reactions of Aryl Benzoates $PhCO_2C_6H_4Y$ (**I–4**) with Potassium Aryloxides $XC_6H_4O^-K^+$ in DMF at 25°C

	k_X (M^{-1} s^{-1})								
	X								
Y	4-MeO	4-Me	3-Me	H	4-Cl	4-Br	3-Br	3-NO_2	4-CN
H	$(1.75 \pm 0.05) \times 10^{-3}$ [a]	9.4×10^{-4} [b]	$(6.4 \pm 0.03) \times 10^{-4}$ [a]						
4-NO_2	2.07×10^3 [b]	3.43×10^3 [b]	5.67×10^3 [b]	3.50×10^3 [b]	5.95×10^2 [b]	4.17×10^2 [b]	1.23×10^2 [b]	9.45[b]	1.19 ± 0.05[a]
3-NO_2	4.04×10^2 [b]	5.06×10^2 [b]	6.38×10^2 [b]	2.75×10^2 [b]	7.70[b]	5.23[b]	1.10 ± 0.03[a]		
4-Cl	1.86[b]	1.36[b]	1.05[b]	0.84 ± 0.02 [a]		0.11 ± 0.01[a]	$(1.7 \pm 0.05) \times 10^{-2}$ [a]		
ρ(Y)[c]	5.47 ± 0.19[d]	6.09 ± 0.28[d]	6.66 ± 0.38[d]	$\rho_{XY} = 5.92 \pm 0.03$[e]		3.31 ± 0.05[f]	3.58 ± 0.05[f]	$\rho_{XY} = 1.63 \pm 0.06$[g]	

[a]The rate constants k_X were calculated by the direct-measurement kinetic method.

[b]The rate constants k_X were calculated using the relative rate constants $k_X/k_{H(3\text{-}Me)}$ taken from Table I.

[c]Y = 4-NO_2, 3-NO_2, 4-Cl.

[d]The parameter ρ^0(Y) is the slope of the plot log k_X versus σ^0(Y) ($r > 0.999$). σ^0(Y) = 0.82 (4-NO_2), 0.27 (4-Cl) [55].

[e]The cross-interaction constant ρ_{XY} is the average of the slopes of the plots ρ^0(Y) versus σ^-(X) ($\rho_{XY} = 5.95 \pm 0.14$, $r > 0.999$) and ρ(X) versus σ^0(Y) ($\rho_{XY} = 5.90 \pm 0.96$, $r > 0.987$) (data are taken from Table I).

[f]The parameter ρ(Y) is the slope of the plot log k_X versus σ^-(Y) ($r > 0.999$).

[g]The cross-interaction constant ρ_{XY} was estimated as the average of the ratios $(\rho(Y)^{3\text{-}Br} - \rho(Y)^{4\text{-}Br})/(\sigma^-(3\text{-}Br) - \sigma^-(4\text{-}Br)) = 1.69$ and $(\rho(X)^{4\text{-}NO2} - \rho(X)^{3\text{-}NO2})/(\sigma^-(4\text{-}NO_2) - \sigma^-(3\text{-}NO_2)) = 1.57$ ($\sigma^-(4\text{-}NO_2) = 1.27$, data are taken from Table I).

the relatively large standard errors of the ρ^0(Y) values (Table II).

Good linear correlations ($r \geq 0.999$) have been obtained in the plots log(k_X) versus σ^-(Y) for the reactions of **1–3** with 3-bromo- and 4-bromophenoxides. The ρ(Y) values are 3.31 and 3.58 at 25°C for 4-bromo- and 3-bromophenoxides, respectively. The low standard errors of ρ(Y) confirm correct use of the common scale of the σ_p^- and σ_m constants of the substituent Y for the reactions of **1–3** with aryloxides with an EWS. As shown in Tables I and II, for the reactions of **1–3** a stronger EWS in aryloxide, $\Delta\sigma^-$(X) > 0 (in the leaving group, $\Delta\sigma^-$(Y) > 0) leads to increase in ρ(Y), $\Delta\rho$(Y) > 0 (in ρ(X) < 0, $\Delta\rho$(X) > 0) and the RSP holds in the both cases. The cross-interaction constant ρ_{XY} has been estimated to be 1.63 at 25°C.

Data of Table II can also be analyzed using the full equation [60],

$$\log(k_{XY}/k_{HH}) = \rho_X\sigma(X) + \rho_Y\sigma(Y) + \sigma_{XY}\sigma(X)\sigma(Y) + c$$

where k_{XY} is the rate constant in the presence of substituents X and Y, k_{HH} is the rate constant when X = Y = H, ρ_X, ρ_Y, and ρ_{XY} are first-derivative sensitivity parameters and the cross-interaction constant, and c is the intercept. The σ^- scale is used for the entering group substituent X, and the σ^0 scale is used for the leaving group substituent Y. It is obvious that $\rho(X) = \rho_X + \rho_{XY}\sigma^0(Y)$ and $\rho^0(Y) = \rho_Y + \rho_{XY}\sigma^-(X)$.

For the reactions of **1–3** with potassium aryloxides with an EDS, the overall correlation coefficient of 0.998 ($n = 9$) is associated with the values of -2.90 ± 1.02 for ρ_X, 7.07 ± 0.30 for ρ_Y, 5.91 ± 1.58 for ρ_{XY}, and -2.01 ± 0.19 for c. For the reactions of **1–3** with potassium 4-bromo- and 3-bromophenoxides, the overall correlation coefficient of 0.999 ($n = 6$) is associated with the values of -5.38 ± 0.37 for ρ_X, 2.94 ± 0.14 for ρ_Y, 1.62 ± 0.44 for ρ_{XY}, and -0.37 ± 0.12 for c.

Therefore, for the reactions of aryl benzoates with potassium aryloxides in DMF, the first-derivative sensitivity parameters ρ_X and ρ_Y values are negative and positive, respectively, and ones decrease as the substituent X changes from EDS to EWS.

It is important to emphasize that the accuracy of the ρ_{XY} value calculated from the full equation is less than that determined from the $\rho(X) - \sigma^0(Y)$ or $\rho^0(Y) - \sigma^-(X)$ dependences. We can confirm that artificial optimizations resulting from statistical treatments of multiple regressions increase the standard error of ρ_{XY} [61].

Isokinetic and Compensation Effects

Each reaction series has been tested in terms of the isokinetic and compensation effects [62–65]. The existence of the isokinetic relationship (IKR) can serve as an argument that the reaction series follow a common mechanism [66–69].

Good linear correlations ($r \geq 0.989$) obtained in the plots of log($k_X/k_{H(3\text{-}Me)}$) versus $1/T$ indicate that all the reactions follow the Arrhenius temperature dependence. The differences in the activation parameters $\Delta\Delta H^{\neq} = \Delta H_X^{\neq} - \Delta H_{H(3-Me)}^{\neq}$ and $\Delta\Delta S^{\neq} = \Delta S_X^{\neq} - \Delta S_{H(3-Me)}^{\neq}$ obtained by use of the Eyring-type equation are summarized in Table I. As shown in Table I, the small magnitudes of $\Delta\Delta H^{\neq}$ and $\Delta\Delta S^{\neq}$ (-1.8 to 4.4 kJ/mol and -10.4 to 21.6 J/(mol·K)) become larger (-24.9 to -18.1 kJ/mol and -150.0 to -82.5 J/(mol·K)) as the substituent X changes from EDS to EWS.

We can conclude that each Hammett reaction series is isokinetic, since the linear plots of log($k_X/k_{H(3\text{-}Me)}$) versus $1/T$ intersect near one point (Table III). The T_{iso} values determined from the log($k_X/k_{H(3\text{-}Me)}$) − $1/T$, $\rho(X) - 1/T$ [70], $\beta_{Nuc} - 1/T$, and log($k_X/k_{H(3\text{-}Me)}$)$_{T2}$ − log($k_X/k_{H(3\text{-}Me)}$)$_{T1}$ [71] dependences differ only slightly (Table III), that is more reliable evidence for the existence of IKR [72].

The statistically correct values of the compensation temperature T_{comp} for isokinetic series determined from the slopes of the plots of $\Delta\Delta H^{\neq}$ versus $\Delta\Delta S^{\neq}$ are also summarized in Table III. A similarity of the T_{comp} and T_{iso} values for each of reaction series indicates that the compensation and isokinetic effects can be synonymous [66].

For all isokinetic series in the current study, the T_{iso} values are positive, so the $\delta\Delta H^{\neq}$ and $\delta\Delta S^{\neq}$ reaction constants have the same sign. The $\delta\Delta H^{\neq}$ and $\delta\Delta S^{\neq}$ reaction constants determined from the dependence of $\Delta H^{\neq}$ and $\Delta S^{\neq}$ activation parameters on the σ substituent constants can be used for the characterization of the electronic and steric effects of the substituents on the reactivity [62–64,72]. Since for all the series the $T_{exp} > T_{iso}$ ratio holds, so the effect of the entering group substituent X on the reactivity is controlled by steric factors [62–65,73]. For this reason, the magnitude of ρ(X) increases with increasing temperature and the RSP fails.

Good linear correlations ($r \geq 0.993$) have been obtained in the plots $\Delta\Delta H^{\neq}$ and $\Delta\Delta S^{\neq}$ versus σ^-(X) for each isokinetic series. The $\delta\Delta H^{\neq}$ and $\delta\Delta S^{\neq}$ values determined from the slopes of the corresponding plots are presented in Table IV. These reaction constants have also been determined from the slopes and intersections, respectively, of the linear plots

Table III Isokinetic Temperatures T_{iso} Determined from Four Dependences and Compensation Temperatures T_{comp} for Reactions of Aryl Benzoates $PhCO_2C_6H_4Y$ (**1–4**) with Potassium Aryloxides $XC_6H_4O^-K^+$ in DMF

		T_{iso} (K)				
Y	X	$\log(k_X/k_{H(3\text{-}Me)}) - 1/T$[a]	$\rho(X) - 1/T$[b]	$\beta_{Nuc} - 1/T$[c]	$\log(k_X/k_{H(3\text{-}Me)})_{T2} - \log(k_X/k_{H(3\text{-}Me)})_{T1}$[d]	T_{comp} (K) $\Delta\Delta H^{\neq} - \Delta\Delta S^{\neq}$[e]
4-NO_2	EDS[f]	209	208	209	209	210
	EWS[g]	70	69	69	73	70
3-NO_2	EDS[h]	234	235	235	234	239
	EWS[i]	114	115	116	119	117
4-Cl	EDS[j]	212	213	213	213	207
H	EDS[k]	99	96	94	104	95

[a] T_{iso} is the temperature of intersection of the plots $\log(k_X/k_{H(3\text{-}Me)}) - 1/T$.

[b] T_{iso} is calculated from the equation $\rho = \text{const}(1 - T_{iso}/T)$.

[c] T_{iso} is calculated from the equation $\beta_{Nuc} = \text{const}(1 - T_{iso}/T)$.

[d] T_{iso} is calculated from the equations $\log(k_X/k_{H(3\text{-}Me)})_{T2} = a + b\log(k_X/k_{H(3\text{-}Me)})_{T1}$ and $T_{iso} = T_2T_1(b-1)/(bT_2 - T_1)$.

[e] T_{comp} is calculated from the equation $\Delta\Delta H^{\neq} = \text{const.} + T_{comp}\Delta\Delta S^{\neq}$.

[f] $T_{iso} = 209$ K $s = 2$; $\rho(X) = (7.35 \pm 0.07) - (1529 \pm 20)/T$ ($r = 0.999$, $s = 0.011$, $n = 4$); $\beta_{Nuc} = -(1.63 \pm 0.02) + (341 \pm 6)/T$ ($r = 0.999$, $s = 0.003$, $n = 4$); $\log(k_X/k_H)_{T2} = (0.068 \pm 0.004) + (1.75 \pm 0.03)$; $\log(k_X/k_H)_{T1}$ for $T_1 = 258$ K, $T_2 = 313$ K ($r = 0.999$, $s = 0.006$, $n = 3$); $\Delta\Delta H^{\neq} = (0.36 \pm 0.04) + (0.210 \pm 0.003) \times 10^3$; $\Delta\Delta S^{\neq}$ ($r = 0.999$, $s = 0.063$, $n = 3$).

[g] $T_{iso} = 70$ K, $s = 2$; $\rho(X) = -(4.38 \pm 0.12) + (302 \pm 34)/T$ ($r = 0.988$, $s = 0.018$, $n = 4$); $\beta_{Nuc} = (0.96 \pm 0.04) - (66 \pm 11)/T$ ($r = 0.973$, $s = 0.006$, $n = 4$); $\log(k_X/k_H)_{T2} = (0.973 \pm 0.006) + (1.07 \pm 0.01)$; $\log(k_X/k_H)_{T1}$ for $T_1 = 258$ K, $T_2 = 313$ K ($r = 0.999$, $s = 0.006$, $n = 3$); $\Delta\Delta H^{\neq} = -(14.45 \pm 0.09) + (0.070 \pm 0.001) \times 10^3$; $\Delta\Delta S^{\neq}$ ($r = 0.999$, $s = 0.037$, $n = 3$).

[h] $T_{iso} = 234$ K, $s = 2$; $\rho(X) = (4.59 \pm 0.12) - (1078 \pm 34)/T$ ($r = 0.999$, $s = 0.018$, $n = 4$); $\beta_{Nuc} = -(1.02 \pm 0.03) + (240 \pm 8)/T$ ($r = 0.999$, $s = 0.004$, $n = 4$); $\log(k_X/k_H)_{T2} = -(0.275 \pm 0.016) + (2.75 \pm 0.08)$; $\log(k_X/k_H)_{T1}$ for $T_1 = 258$ K, $T_2 = 313$ K ($r = 0.999$, $s = 0.005$, $n = 3$); $\Delta\Delta H^{\neq} = -(0.75 \pm 0.02) + (0.239 \pm 0.002) \times 10^3$; $\Delta\Delta S^{\neq}$ ($r = 0.999$, $s = 0.019$, $n = 3$).

[i] $T_{iso} = 114$ K, $s = 1$; $\rho(X) = -(6.96 \pm 0.28) + (802 \pm 79)/T$ ($r = 0.990$, $s = 0.042$, $n = 4$); $\beta_{Nuc} = (1.56 \pm 0.06) - (181 \pm 16)/T$ ($r = 0.992$, $s = 0.008$, $n = 4$); $\log(k_X/k_H)_{T2} = -(0.484 \pm 0.007) + (1.15 \pm 0.01)$; $\log(k_X/k_H)_{T1}$ for $T_1 = 258$ K, $T_2 = 313$ K ($r = 0.999$, $s = 0.003$, $n = 3$); $\Delta\Delta H^{\neq} = -(7.50 \pm 0.12) + (0.117 \pm 0.001) \times 10^3$; $\Delta\Delta S^{\neq}$ ($r = 0.999$, $s = 0.023$, $n = 3$).

[j] $T_{iso} = 212$ K, $s = 3$; $\rho(X) = -(4.30 \pm 0.09) + (916 \pm 27)/T$ ($r = 0.999$, $s = 0.012$, $n = 4$); $\beta_{Nuc} = (0.94 \pm 0.04) - (200 \pm 11)/T$ ($r = 0.997$, $s = 0.005$, $n = 4$); $\log(k_X/k_H)_{T2} = -(0.077 \pm 0.005) + (1.59 \pm 0.02)$; $\log(k_X/k_H)_{T1}$ for $T_1 = 273$ K, $T_2 = 328$ K ($r = 0.999$, $s = 0.003$, $n = 3$); $\Delta\Delta H^{\neq} = -(0.49 \pm 0.01) + (0.207 \pm 0.001) \times 10^3$; $\Delta\Delta S^{\neq}$ ($r = 0.999$, $s = 0.011$, $n = 3$).

[k] $T_{iso} = 99$ K, $s = 4$; $\rho(X) = -(3.25 \pm 0.04) + (313 \pm 13)/T$ ($r = 0.998$, $s = 0.004$, $n = 4$); $\beta_{Nuc} = (0.72 \pm 0.01) - (68 \pm 2)/T$ ($r = 0.999$, $s = 0.001$, $n = 4$); $\log(k_X/k_H)_{T2} = 1.07$; $\log(k_X/k_H)_{T1}$ for $T_1 = 298$ K, $T_2 = 343$ K ($r = 1.000$, $s = 0.001$, $n = 3$); $\Delta\Delta H^{\neq} = (0.01 \pm 0.02) + (0.095 \pm 0.002) \times 10^3$; $\Delta\Delta S^{\neq}$ ($r = 0.999$, $s = 0.019$, $n = 3$).

$\rho(X)$ versus $1/T$. The results obtained by independent ways are close, so a validity of the $\delta\Delta H^{\neq}$ and $\delta\Delta S^{\neq}$ values are confirmed. Table IV also contains the previously published data for the reactions of **5** with potassium aryloxides in DMF [49]. The negative $\delta\Delta H^{\neq}$ and $\delta\Delta S^{\neq}$ values obtained for all the reaction series except those of **1** and **2** with potassium aryloxides with an EDS indicate that the activation parameters $\Delta H^{\neq}$ and $\Delta S^{\neq}$ decrease with decreasing the nucleophilicity of aryloxides.

Mechanism of Reactions of Aryl Benzoates with Potassium Aryloxides in DMF

In the generally accepted stepwise mechanism of acyl transfer reactions, a nucleophile attacks at the carbonyl carbon pushing the π bond electrons up onto the oxygen to give a tetrahedral intermediate [74]. Three reaction mechanisms can be proposed for the *spiro*-σ-complex formation: (1) the addition of aryloxide at the carbonyl carbon to yield a tetrahedral intermediate T, followed by the intramolecular cyclization; (2) the intramolecular cyclization of aryl benzoate, generating a zwitterionic Meisenheimer complex, which eventually reacts with aryloxide; (3) the addition of aryloxide and the intramolecular cyclization proceed concertedly. One can suggest that the first and latter mechanisms are the most plausible.

The large $\rho^0(Y)$ values for the reaction series of **1–3** with aryloxides with an EDS indicate that the *spiro*-σ-complex formation should be referred to the nucleophilic aromatic substitution, i.e., the intramolecular cyclization of T is the RDS (Scheme 2). As evidence, the magnitude of $\rho^0(Y)$ for the reactions of 4-Y-2,6-dinitrochlorobenzene (Y = NO_2, CN, CF_3) with benzylamines in MeCN are in the range of 6.25−6.43 [75]. A similar $\rho^0(Y)$ value has been obtained for the reactions of 4-Y-2-nitrochlorobenzene (Y = OMe, Me, H, Cl, CO_2Me, COMe, NO_2) with 4-methylthiophenoxide in DMF at 25°C [76]. The large positive ρ_{XY} also is

Table IV Reaction Constants $\delta\Delta H^{\neq}$ and $\delta\Delta S^{\neq}$ for Reactions of Aryl Benzoates $PhCO_2C_6H_4Y$ (**1–4**) and 2,4-Dinitrophenyl Benzoate (**5**) with Potassium Aryloxides $XC_6H_4O^-K^+$ in DMF

	X					
	$\delta\Delta H^{\neq}$ (kJ/mol)[a]		$\delta\Delta S^{\neq}$ (J/(mol·K))[b]		T_{iso} (K)[c]	
Y	EDS	EWS	EDS	EWS	EDS	EWS
4-NO_2	29.5[d,k] (29.3)	−5.8[e] (−5.8)	140.5[d,k] (140.7)	−83.8[e] (−83.9)	209	70
3-NO_2	21.0[f,k] (20.6)	−15.5[g] (−15.4)	88.0[f,k] (87.9)	−132.9[g] (−133.3)	234	114
4-Cl	−17.0[h,k] (−17.5)		−82.0[h,k] (−82.3)		212	
H	−6.0[i] (−6.0)		−63.0[i] (−62.2)		99	
2,4-$(NO_2)_2$[j]	−21.0	−36.9	−61.5	−185.1	345	215

[a] $\delta\Delta H^{\neq}$ is the slope of the plot $\Delta\Delta H^{\neq}$ versus. σ^-(X). Data in the brackets are obtained from the dependence $\rho - 1/T$ (Table III).

[b] $\delta\Delta S^{\neq}$ is the slope of the plot $\Delta\Delta S^{\neq}$ versus. σ^-(X). Data in the brackets are obtained from the dependence $\rho - 1/T$ (Table III).

[c] Data are taken from Table III.

[d] $\Delta\Delta H^{\neq} = (6.1 \pm 0.2) + (29.5 \pm 0.7)\sigma^-$(X) ($r = 0.999$, $s = 0.122$, $n = 3$); $\Delta\Delta S^{\neq} = (27.4 \pm 0.4) + (140.5 \pm 2.0)\sigma^-$(X) ($r = 0.999$, $s = 0.286$, $n = 3$).

[e] $\Delta\Delta H^{\neq} = -(19.1 \pm 0.2) - (5.8 \pm 0.3)\sigma^-$(X) ($r = 0.999$, $s = 0.147$, $n = 3$); $\Delta\Delta S^{\neq} = -(67.0 \pm 1.9) - (83.8 \pm 2.7)\sigma^-$(X) ($r = 0.999$, $s = 1.585$, $n = 3$).

[f] $\Delta\Delta H^{\neq} = (5.9 \pm 0.0) + (21.0 \pm 0.0)\sigma^-$(X) ($r = 1$, $s = 0$, $n = 3$); $\Delta\Delta S^{\neq} = (27.7 \pm 0.1) + (88.0 \pm 0.6)\sigma^-$(X) ($r = 0.999$, $s = 0.082$, $n = 3$).

[g] $\Delta\Delta H^{\neq} = -(15.1 \pm 0.0) - (15.5 \pm 0.1)\sigma^-$(X) ($r = 0.999$, $s = 0.015$, $n = 3$); $\Delta\Delta S^{\neq} = -(65.3 \pm 0.1) - (132.9 \pm 0.4)\sigma^-$(X) ($r = 1$, $s = 0.062$, $n = 3$).

[h] $\Delta\Delta H^{\neq} = -(1.7 \pm 0.2) - (17.0 \pm 1.2)\sigma^-$(X) ($r = 0.998$, $s = 0.163$, $n = 3$); $\Delta\Delta S^{\neq} = -(5.6 \pm 1.0) - (82.0 \pm 5.2)\sigma^-$(X) ($r = 0.998$, $s = 0.735$, $n = 3$).

[i] $\Delta\Delta H^{\neq} = -(0.5 \pm 0.1) - (6.0 \pm 0.6)\sigma^-$(X) ($r = 0.995$, $s = 0.082$, $n = 3$); $\Delta\Delta S^{\neq} = -(4.8 \pm 1.4) - (63.0 \pm 7.5)\sigma^-$(X) ($r = 0.993$, $s = 1.061$, $n = 3$).

[j] Data are taken from [49].

[k] $\delta\Delta H^{\neq} = (-39.9 \pm 1.0) + (85.1 \pm 1.5)\sigma^0$(Y) ($r = 0.999$, $s = 0.617$, $n = 3$); $\delta\Delta S^{\neq} = (-190.8 \pm 9.7) + (399.4 \pm 15.0)\sigma^0$(Y) ($r = 0.999$, $s = 6.172$, $n = 3$).

in line with the rate-limiting formation of a Meisenheimer complex. The cross-interaction constant ρ_{XY} for the reactions of 4-Y-2,6-dinitrochlorobenzene (Y = NO_2, CN, CF_3) with pyridines in MeCN is 3.95 at 25°C [77].

According to Scheme 2, the rate constant k_X is effective and contains the equilibrium constant K_1 of the first fast step and the rate constant k_2 of the second RDS. Then, $\Delta H^{\neq} = \Delta H_1^0 + \Delta H_2^{\neq}$ and $\Delta S^{\neq} = \Delta S_1^0 + \Delta S_2^{\neq}$, where ΔH_1^0, $\Delta H_2^{\neq} > 0$ and ΔS_1^0, $\Delta S_2^{\neq} < 0$ [63–65]. We believe that T is relatively stable, so ΔH_1^0 and ΔS_1^0 are insignificantly dependent of the substituents, and, hence, the reaction constants $\delta\Delta H^{\neq}$ and $\delta\Delta S^{\neq}$ obtained for reaction series of **1–3** with aryloxides with an EDS are a good approximation to $\delta\Delta H_2^{\neq}$ and $\delta\Delta S_2^{\neq}$.

As a rule, the reaction constants $\delta\Delta H^{\neq}$ and $\delta\Delta S^{\neq}$ are formally divided into internal and external terms, which are related to the reaction and the solvation, respectively [63–65]. The external term influences markedly the value of $\delta\Delta H^{\neq}$, and it determines the value of $\delta\Delta S^{\neq}$ for the reaction series of substituted carboxylic esters with an anionic nucleophile in water or solvent mixtures containing water [63–65]. It can be explained by the significant difference between the substituent effect on the solvation of the neutral substrate and that of the anionic transition state. However, for the anionic T and TS (transition state) this difference in DMF should not be essential, and so the solvent effect on $\delta\Delta H_2^{\neq}$ and $\delta\Delta S_2^{\neq}$ (as well as $\delta\Delta H^{\neq}$ and $\delta\Delta S^{\neq}$) is insignificant.

Generally speaking, the linear dependence of $\delta\Delta H^{\neq}$ (i.e., $\Delta H_2^{\neq}$) on the σ^- constant of the entering group substituent X indicates that the TS formation can be considered in the terms of the electrostatic bonding [78] between the aryloxide oxygen (the O-reaction center) and the carbon at the ipso position in the leaving group (the C-reaction center), which is accompanied by an entropy decrease due to forming 1,3-dioxetane ring.

Williams et al. studied in detail associations between two or more molecules where the electrostatic interactions play an important role [78]. The monotonic dependence of the enthalpic benefit on the entropic cost is typical of associations, and it can be the cause of the enthalpy–entropy compensation [78]. We employed this type of monotonicity to interpret the compensation effect observed for the studied reactions

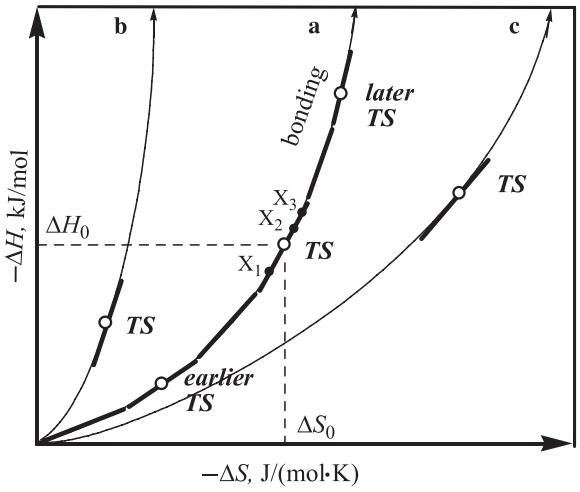

Figure 3 An enthalpy–entropy diagram for the reacting bond. The general form of the curves a–c is defined by the monotonic dependence of the enthalpic benefit on the entropic cost in a simple exothermic bimolecular association [78]. The upper limit determines a covalent bond. Series of tangent line segments approximate the curve a. The electrostatic bonding in the point (ΔH_0, ΔS_0) is the same as in TS. Three points on this tangent line segment refer to variation of the entering group substituents X_1, X_2, and X_3, and the coordinates of these points can be obtained from the following equations: $\Delta H(X) = \Delta H_0 + \delta\Delta H^{\neq}\cdot\sigma^-(X)$ and $\Delta S(X) = \Delta S_0 + \delta\Delta S^{\neq}\cdot\sigma^-(X)$, where ΔH_0 and ΔS_0 are related to the unsubstituted nucleophile, the ratio $\delta\Delta H^{\neq}/\delta\Delta S^{\neq}$ are T_{comp}. The curvature of the curve depends on the tightness of the TS structure; the curves b and c refer to tighter and looser structures of TS, respectively.

(Fig. 3). According to the general form of the curve a, every point on it has a different slope. The slope changes all along the curve a, and so it can be taken as a measure of the electrostatic bonding. The original curve a can be approximated by series of tangent line segments. It is very important that the slope of a point on the curve a is the slope of the tangent line segment at this point. One of these segments is tangent at the point in which the electrostatic bonding is the same as in TS. As shown in Fig. 3, ΔH_0 and ΔS_0 are the coordinates of the corresponding point.

In line with this model, the existence of the excellent compensation effect for reaction series implies that a variation of TS with the substituents X_1, X_2, and X_3 can be well approximated by a tangent line segment at the point (ΔH_0, ΔS_0) whose slope is equal to T_{comp}. For these substituents, the terms of the activation parameters referring to the electrostatic bonding are linearly dependent on the $\sigma^-(X)$ substituent constants, i.e., $\Delta H(X) = \Delta H_0 + \delta\Delta H^{\neq}\cdot\sigma^-(X)$ and $\Delta S(X) = \Delta S_0 + \delta\Delta S^{\neq}\cdot\sigma^-(X)$, where ΔH_0 and ΔS_0 are related to unsubstituted nucleophile, the ratio $\delta\Delta H^{\neq}/\delta\Delta S^{\neq}$ are T_{comp}. Then, $\Delta H_2^{\neq}(X) = \Delta H_i^{\neq} + \Delta H_0 + \delta\Delta H^{\neq}\cdot\sigma^-(X)$ and $\Delta S_2^{\neq}(X) = \Delta S_i^{\neq} + \Delta S_0 + \delta\Delta S^{\neq}\cdot\sigma^-(X)$, where $\Delta H_i^{\neq}$ and $\Delta S_i^{\neq}$ are the terms of the activation parameters, which do not depend on the electrostatic bonding. Obviously, van't Hoff (Arrhenius) lines describing the kinetics of this reaction series, $\Delta G_2^{\neq}(X) = \Delta H_2^{\neq}(X) - T\Delta S_2^{\neq}(X)$ ($\log k_X = \log A(X) - E_a(X)/RT$), should intersect at the temperature T_{comp}, and then, the compensation and isokinetic effects can be synonymous.

We believe that the TS motion along the reaction coordinate in the direction of the *spiro*-σ-complex (a normal Hammond effect) leads to increase the electrostatic bonding between the reaction centers, and, hence, increase the slope of the corresponding tangent line segment. Then, the isokinetic temperature T_{iso} as well as the compensation temperature T_{comp} can be interpreted in the terms of the transition state position along the reaction coordinate: the larger the corresponding value, the later the transition state.

It should be emphasized that the existence of the isokinetic effect is unlikely in the case of the strong substituent effect on the electrostatic bonding. However, the compensation effect can be operative because a statistical criterion to judge its existence is less correct. As a rule, the transition state structure and, hence, the reacting bond do not vary significantly with variation of the substituents in the nucleophile [2], and such a reaction series is isokinetic. At the same time, the T_{iso} values obtained for reaction series of **1–3** with potassium aryloxides with an EDS are close, 209, 234, and 212 K, respectively, and it means that the TS structure remains essentially constant despite changing the leaving group substituent Y from 4-NO_2 to 3-NO_2 and 4-Cl (Table IV). The $\delta\Delta H^{\neq}$ and $\delta\Delta S^{\neq}$ values for the corresponding series range from 29.5 to 21 and –17 kJ/mol and from 140.5 to 88 and –82 J/(mol·K), respectively, i.e., they strongly decrease with reducing the electron-withdrawing ability of the substituent Y.

The positive $\delta\Delta H^{\neq}$ and $\delta\Delta S^{\neq}$ values obtained for the reactions of **1** and **2** with potassium aryloxides with an EDS are typical of the nucleophilic substitution reactions in which the entering group substituent is varied. For the reactions of 2-chloro-3-nitro- and 2-chloro-5-nitro-pyridines with aryloxides in MeOH proceeded through the formation of a Meisenheimer complex the reaction constants are also positive [79].

On the other hand, the negative $\delta\Delta H^{\neq}$ and $\delta\Delta S^{\neq}$ values for the corresponding reaction series of **3** can attribute only to the effect of the substituent X on the electrophilic center. These results are in a good agreement with the TS structure in which the entering group substituent X oppositely influences the O- and C-reaction

centers. Good linear correlations ($r \geq 0.999$) have been obtained in the plots $\delta\Delta H^{\neq}$ and $\delta\Delta S^{\neq}$ versus σ^0(Y) (Table IV). The negative intercepts of the corresponding plots, −39.9 kJ/mol and −190.8 J/(mol·K), indicate that the substituent sensitivity of the C-reaction center is larger than that of the O-reaction center, and it is in line with the RSP. On the other hand, the positive slopes of the plots, 85.1 kJ/mol and 399.4 J/(mol·K), mean that an EWS in the leaving group increasing the positive charge on the C-reaction center decreases its substituent sensitivity. It is interesting that the $\delta\Delta H^{\neq}$ and $\delta\Delta S^{\neq}$ values are close to zero when $\sigma^0(\mathrm{Y}) \sim 0.47$.

The T_{iso} value for reactions of **5** with potassium aryloxides with an EDS has been determined to be 345 K. One can suggest that TS becomes later as the substituent Y changes the position in the leaving group from para (or meta) to ortho. At the same time, the negative $\delta\Delta H^{\neq}$ and $\delta\Delta S^{\neq}$ values, –21 kJ/mol and –61.5 J/(mol·K), obtained for the reaction series of **5** with potassium aryloxides with an EDS indicate the small positive charge on the C-reaction center, i.e., the decreased C_{Ar}–O bond order. The $\delta\Delta H^{\neq}$ and $\delta\Delta S^{\neq}$ values, –6.0 kJ/mol and –63.0 J/(mol ·K), obtained for the reaction series of the unsubstituted substrate (**4**) are greater than those for the corresponding reactions of the substrate with a weak EWS (**3**). and it supports the increased C_{Ar}–O bond order. The lower T_{iso} value, 99 K, obtained for the reactions of **4** with potassium aryloxides with an EDS is also in line with this assumption.

To explain such changes in the TS structure, the one-dimensional reaction coordinate is not sufficient. Therefore, we employed two-dimensional reaction coordinate diagram, also known as the More O'Ferrall–Jencks diagram [80,81]. In two-dimensional reaction coordinate diagram shown in Fig. 4a, the reactants are depicted in the lower left corner, the *spiro*-σ-complex in the upper right corner, the symmetric tetrahedral intermediate in the lower right corner, and the zwitterionic intermediate in the upper left corner. The C_{Ar}–O bond formation proceeds along the *y* axis and the C–O bond formation proceeds along the *x* axis. The reaction pathway representing a stepwise process traverses near the edges of the More O'Ferrall–Jencks diagram. The transition state TS for the rate-determining intramolecular cyclization of the intermediate T is located at a saddle point on the right-hand limb of pathway.

We believe that the EWS in the leaving group stabilizes the *spiro*-σ-complex and destabilizes the symmetric tetrahedral intermediate [82], so TS moves along the reaction coordinate toward the lower right corner decreasing the C_{Ar}–O bond order (a normal Hammond effect). One can suggest that if the TS motion along the reaction coordinate were dominant the T_{iso} value would decrease. However, the T_{iso} value has been found to significantly increase when the substrate changes from **4** to **1–3**. It means that the TS motion can be discussed in terms of two vectors, one along the reaction coordinate and one perpendicular to it. Since the zwitterionic intermediate shown in Fig. 4a can be considered as an acylium cation, so the upper left corner should become much less stable than the lower right corner with the EWS in the leaving group. Such a destabilization of the zwitterionic intermediate should cause the TS motion perpendicular to the reaction coordinate toward the lower right corner (an *anti*-Hammond effect [83]) increasing the tightness of the TS structure [84]. We believe that the tightness of the TS structure determines the curvature of the dependence $\Delta H - \Delta S$ for the reacting bond just as the strength of the electrostatic bonding determines the slope of the tangent line segment: the tighter the TS, the larger the curvature (curves **a**-**b** in Fig. 3). The fact that the T_{iso} value (i.e., the slope of the tangent line segment) increases despite decreasing the C_{Ar}–O bond order means that in this case the change in the tightness of the TS structure is dominant (Fig. 3).

It is important to emphasize that the T_{iso} value changes depending on normal and *anti*-Hammond effects, and hence, incorrect use of the isokinetic temperature T_{iso} to interpret the reaction mechanism can lead to false conclusions.

Using the corresponding approach for the reaction series of **5** with aryloxides with an EDS, we can conclude that if the nitro group is added at the ortho position in the leaving group, the transition state TS will move along and perpendicular to the reaction coordinate toward the symmetric tetrahedral intermediate (Fig. 4).

We believe that variation of the entering group substituent X also affects the TS structure. Since an EDS in the entering group destabilizes the *spiro*-σ-complex and stabilizes the symmetric tetrahedral intermediate, but an EWS stabilizes the first and destabilizes the latter, so the lower right corner becomes less stable than the upper right corner when the substituent X changes from EDS to EWS. This effect move TS along the reaction coordinate toward lower right corner, i.e., TS becomes earlier (Fig. 4a). In contrast to variation of the leaving group substituent Y, one of the entering group substituent X has a little effect the upper left corner, and hence, the TS motion along the reaction coordinate is dominant. In line with this conclusion, the T_{iso} value decreases as the substituent X changes from EDS to EWS, from 209 to 70 K for **1**, from 234 to 114 K for **2**, and from 345 to 215 K for **5** (Table IV). The negative $\delta\Delta H^{\neq}$ and $\delta\Delta S^{\neq}$ values for reactions of **1**, **2** with potassium aryloxides with an EWS, –5.8 kJ/mol and –83.8 J/(mol·K) for **1** and –15.5 kJ/mol and

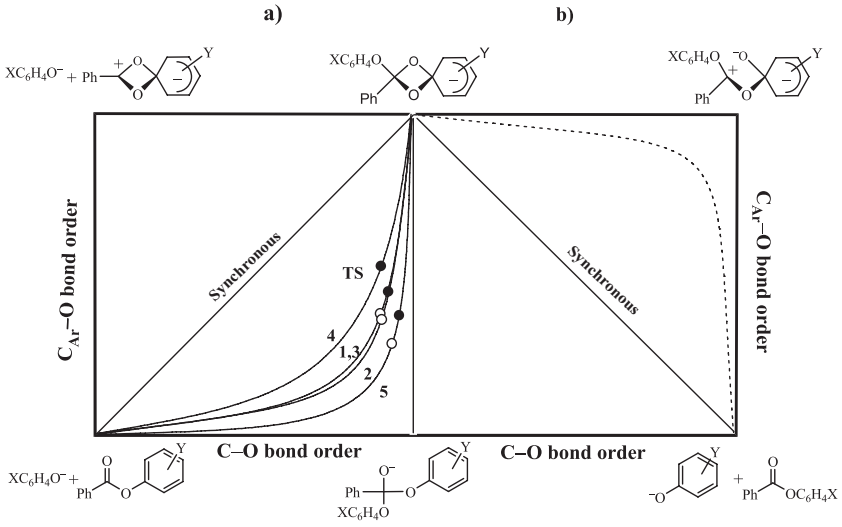

Figure 4 More O'Ferrall–Jencks diagrams for the four-step mechanism of the reactions of aryl benzoates with potassium aryloxides in DMF: the left diagram (a) for the stepwise *spiro*-σ-complex formation; the right diagram (b) for the stepwise *spiro*-σ-complex breakdown. In the left diagram, the positions of TS for the reactions of **1–5** with potassium aryloxides with an EDS and **1–3**, **5** with potassium aryloxides with an EWS are represented by points (•) and (o), respectively. (See the text for discussion.)

–132.9 J/(mol·K) for **2,** support a decrease in the C_{Ar}–O bond order. The large negative $\delta\Delta H^{\neq}$ and $\delta\Delta S^{\neq}$ values for reactions of **5** with potassium aryloxides with an EWS, –36.9 kJ/mol and –185.1 J/(mol·K), also indicate the earlier TS (Table IV). A direct resonance interaction of the substituent Y with the C-reaction center in TS for the reactions of **1–3** with potassium aryloxides with an EWS implies that a small negative charge is delocalized in the leaving group. The small ρ(Y) and ρ_{XY} values for the corresponding reactions series support this conclusion.

It is interesting to note that the ρ(Y) and ρ_{XY} values for these reactions are similar to that for the reactions of aminolysis and pyridinolysis of aryl esters and their thiol, thiono, and dithio derivatives in MeCN proceeding through the rate-limiting breakdown of a zwitterionic tetrahedral intermediate [85–88].

Thus, broken $\Delta\Delta H^{\neq}$ and $\Delta\Delta S^{\neq}$ versus σ^{-}(X) plots for the substrates **1, 2**, **5** can be interpreted in the terms of change in the TS position along the reaction coordinate. In the protic solvent, it refers to changes in the solvation with the electronic effect of the substituents [63–65].

Employing the proposed approach for the reactions of **1** and **5** with potassium aryloxides with an EWS, one can conclude that TS moves along and perpendicular to the reaction coordinate toward the symmetric tetrahedral intermediate as the leaving group substituent Y changes from 4-NO_2 to 2,4-$(NO_2)_2$ (Table IV). Surprisingly, the same conclusion can be drawn when the substituent Y changes from 4-NO_2 to 3-NO_2. However, the magnitude of the meta effect is much smaller than that of the ortho effect. The weaker meta effect can be observed for the reaction of aryl benzoates with potassium aryloxides with an EDS, i.e., one becomes apparent for the earlier TS.

Thus, for all isokinetic series of the reactions of aryl benzoates with potassium aryloxides in DMF, the RDS is the *spiro*-σ-complex formation. It is evident that the mechanism of the *spiro*-σ-complex breakdown formally refers to a [2+2] retro-cycloaddition, and hence it should proceed through a zwitterionic intermediate [89]. Such an intermediate will be formed only if the C–O bond in the 1,3-dioxetane cycle breaks. The departure of the leaving group from this zwitterionic intermediate leads to products.

As shown in Fig. 4b, in two-dimensional reaction coordinate diagram of the *spiro*-σ-complex breakdown, the products are depicted in the lower right corner, the *spiro*-σ-complex in the upper left, and the symmetric tetrahedral intermediate in the lower left. In the upper right corner of this system, there is the zwitterionic intermediate. The reaction pathway traversing near the edges of the More O'Ferrall–Jencks diagram represents a stepwise process involving the zwitterionic intermediate.

Therefore, the mechanism proposed for the reactions of aryl benzoates with potassium aryloxides in DMF includes four steps. We believe that the delocalization of the negative charge in the leaving group

stabilizes TS compared to the transition states of the formation and breakdown of the symmetric tetrahedral intermediate, respectively, and so, the four-step mechanism is preferred. However, in a protic solvent the stabilizing solvation of TS should be smaller than that of the corresponding transition states of the formation and breakdown of the symmetric tetrahedral intermediate, and then, the $A_N + D_N$ mechanism can compete with the four-step mechanism.

Um et al. have suggested that the reactions of **1** with aryloxides in absolute ethanol and DMSO–H_2O mixture at 25°C proceed through the stepwise mechanism with the formation of the symmetric tetrahedral intermediate [55,57]. Comparison of the rate constants shows that the reactions of **1** with potassium aryloxides in DMF are much faster than that in absolute ethanol or DMSO–H_2O mixture. For example, the rate constant $k_{4\text{-CN}}$ for the reaction of **1** with potassium 4-cyanophenoxide in DMF was determined to be 1.19 M^{-1} s^{-1} at 25°C and it is ∼700 times faster than that in the absolute ethanol [55]. We can conclude that the reactants and tetrahedral intermediate are strongly stabilized as a solvent changes from DMF (aprotic) to absolute ethanol or DMSO–H_2O mixture (protic), so the reaction mechanism changes and the rate constants decrease.

It should be emphasized that the proposed mechanism is realized provided that the pK_a values of the entering aryloxides are larger than that of the leaving aryloxides. In line with the principle of the microscopic reversibility [90,91], the mechanism of the reverse reactions also includes four steps: (1) a nucleophilic attack of the carbonyl oxygen of aryl benzoates at the ipso position in potassium aryloxide, followed by (2) the intramolecular cyclization leading to formation of the *spiro-σ*-complex, (3) the spiro ring opening with yielding the tetrahedral intermediate T and then, (4) the departure of the leaving group. One can suggest that the reactions of **3** with potassium aryloxides with an EWS proceed according to this mechanism. Since good linear correlations ($r \geq 0.999$) have been obtained in the plots $\log(k_X)$ versus $\sigma^-(Y)$ for the reactions of **1–3** with 3-bromo- and 4-bromophenoxides, so for the corresponding reactions of **3** the third step is the RDS.

CONCLUSIONS

We have shown in the present study that the approach based on analysis of the effect of the entering group substituent on the activation parameters gives significant information regarding the transition state structure of the RDS and its position on the two-dimensional reaction coordinate diagram. Our result in general indicated that the reactions of aryl benzoates with potassium aryloxides in DMF proceed via the four-step mechanism involving (1) the nucleophilic attack of aryloxide at the carbonyl carbon generating the tetrahedral intermediate T, (2) the intramolecular nucleophilic attack of the alkyloxide at the ipso position in the leaving group leading to formation of the *spiro-σ*-complex, (3) the spiro ring opening with yielding the zwitterionic intermediate, and (4) the departure of the leaving group. The second step is the RDS, i.e., the reactions of aryl benzoates with potassium aryloxides in DMF, refer to a nucleophilic aromatic substitution. The origin of the breaks in the Hammett plots can be explained by the TS motion along the reaction coordinate according to a Hammond effect. The reaction mechanism can change from four steps to $A_N + D_N$ when the solvent changes from DMF to protic ones.

BIBLIOGRAPHY

1. Bourne, N.; Chrystiuk, E.; Davis, A. M.; Williams, A. J Am Chem Soc 1988, 110, 1890–1895.
2. Buncel, E.; Um, I. H.; Hoz, S. J Am Chem Soc 1989, 111, 971–975.
3. Pregal, M.; Dunn, E. J.; Buncel, E. J Am Chem Soc 1991, 113, 3545–3550.
4. Hengge, A. J Am Chem Soc 1992, 114, 6575.
5. Williams, A. Adv Phys Org Chem 1992, 27, 1–55.
6. Stefanidis, D.; Cho, S.; Dhe-Paganon, S.; Jencks, W. P. J Am Chem Soc 1993, 115, 1650–1656.
7. Hengge, A.; Hess, R. A. J Am Chem Soc 1994, 116, 11256–11257.
8. Hengge, A.; Eadens, W. A.; Elsing, H. J Am Chem Soc 1994, 116, 5045–5049.
9. Williams, A. Chem Soc Rev 1994, 23, 93–100.
10. Tarkka, R. M.; Buncel, E. J Am Chem Soc 1995, 117, 1503–1507.
11. Colthurst, M. J.; Williams, A. J Chem Soc, Perkin Trans 2 1997, 1493–1497.
12. Fernandez, M. A.; Rossi, R. H. J Org Chem 1999, 64, 6000–6004.
13. Williams, A. Concerted Organic and Bio-organic Mechanisms; CRC Press: Boca Raton, FL, 2000; Ch. 4, pp. 43–46.
14. Lee, H. W.; Yun, Y. S.; Lee, B. S.; Koh, H. J.; Lee, I. J Chem Soc, Perkin Trans 2 2000, 2302–2305.
15. Andres, G. O.; Granados, A. M.; Rossi, R. H. J Org Chem 2001, 66, 7653–7657.
16. Um, I. H.; Han, H. J.; Ahn, J. A.; Kang, S.; Buncel, E. J Org Chem 2002, 67, 8475–8480.
17. Hengge, A. Acc Chem Res 2002, 35, 105–112.
18. Castro, E. A.; Pavez, P.; Santos, J. G. J Org Chem 2001, 66, 3129–3132.
19. Castro, E. A.; Pavez, P.; Santos, J. G. J Org Chem 2003, 68, 3640–3545.

20. Castro, E. A.; Arellano, D.; Pavez, P.; Santos, J. G. J Org Chem 2003, 68, 9034–9039.
21. Castro, E. A.; Andujar, M.; Toro, A.; Santos, J. G. J Org Chem 2003, 68, 3608–3613.
22. Castro, E. A.; Aguayo, R.; Santos, J. G. J Org Chem 2003, 68, 8157–8161.
23. Lee, I.; Lee, H. W.; Yu, Y. K. Bull Korean Chem Soc 2003, 24, 993–998.
24. Castro, E. A.; Aliaga, M.; Santos, J. G. J Org Chem 2004, 69, 6711–6714.
25. Oh, H. K.; Park, J. E.; Sung, D. D.; Lee, I. J Org Chem 2004, 69, 9285–9288.
26. Oh, H. K.; Park, J. E.; Sung, D. D.; Lee, I. J Org Chem 2004, 69, 3150–3153.
27. Oh, H. K.; Ha, J. S.; Sung, D. D.; Lee, I. J Org Chem 2004, 69, 8219–8223.
28. Um, I.-H.; Lee, J. Y.; Kim, H. T.; Bae, S. K. J Org Chem 2004, 69, 2436–2441.
29. Um, I. H.; Kim, K. H.; Park, H. R.; Fujio, M.; Tsuno, Y. J Org Chem 2004, 69, 3937–3942.
30. Um, I.-H.; Lee, J. Y.; Lee, H. W.; Nagano, Y.; Fujio, M.; Tsuno, Y. J Org Chem 2005, 70, 4980–4987.
31. Um, I.-H.; Hong, J. Y.; Seok, J. A. J Org Chem 2005, 70, 1438–1444.
32. Castro, E. A.; Gazitua, M.; Santos, J. G. J Org Chem 2005, 70, 8088–8092.
33. Castro, E. A.; Aguayo, R.; Bessolo, J.; Santos, J. G. J Org Chem 2005, 70, 7788–7791.
34. Castro, E. A.; Aguayo, R.; Bessolo, J.; Santos, J. G. J Org Chem 2005, 70, 3530–3536.
35. Um, I.-H.; Lee, J. Y.; Bae, S. Y.; Buncel, E. Can J Chem 2005, 83, 1365–1371.
36. Um, I.-H.; Kim, E. Y.; Park, H.-R.; Jeon, S.-E. J Org Chem 2006, 71, 2302–2306.
37. Um, I.-H.; Hwang, S. J.; Baek, M. H.; Park, H.-R. J Org Chem 2006, 71, 9191–9197.
38. Um, I.-H.; Lee, J. Y.; Ko, S. H.; Bae, S. K. J Org Chem 2006, 71, 5800–5803.
39. Castro, E. A.; Echevarria, G. R.; Opazo, A.; Robert, P.; Santos, J. G. J Phys Org Chem 2006, 19, 129–135.
40. Um, I.-H.; Lee, J. Y.; Lee, H.W; Fujio, M.; Tsuno, Y. Org Biomol Chem 2006, 4, 2979–2985.
41. Um, I.-H.; Hwang, S. J.; Buncel, E. J Org Chem 2006, 71, 915–920.
42. Um, I.-H.; Park, Y.-M.; Fujio, M.; Mishima, M.; Tsuno, Y. J Org Chem 2007, 72, 4816–4821.
43. Castro, E. A.; Ramos, M.; Santos, J. G. J Org Chem 2009, 74, 6374–6377.
44. Castro, E. A.; Aliaga, M.; Campodónico, P. R.; Cepeda, M.; Contreras, R.; Santos, J. G. J Org Chem 2009, 74, 9173–9179.
45. Castro, E. A.; Milan, D.; Aguayo, R.; Campodónico, P. R.; Santos, J. G. Int J Chem Kinet 2011, 44, 687–693.
46. Ośkina, I. A.; Vlasov, V. M. Org Chem 2009, 45, 523–527.
47. Ośkina, I. A.; Vlasov, V. M. Russ J Org Chem 2010, 46, 326–330.
48. Khalfina, I. A.; Vlasov, V. M. Russ J Org Chem 2008, 44, 1619–1626.
49. Khalfina, I. A.; Vlasov, V. M. Russ J Org Chem 2011, 47, 845–854.
50. Vogel, A. T. Practical Organic Chemistry; Longman's Green: London, 1962.
51. Kornblum, N.; Lurie, A. P. J Am Chem Soc 1959, 81, 2705–2715.
52. Seo, J. A.; Kim, S. I.; Hong, Y. J.; Um, I. H. Bull Korean Chem Soc 2010, 31, 303–308.
53. Hansch, C.; Leo, A.; Taft, R. W. Chem Rev 1991, 91, 165–195.
54. Kepka, C.; Penhoat, M.; Barbry, D.; Rolando, Ch. In 13th International Electronic Conference on Synthetic Organic Chemistry (ECSOC-13), November 1–30, 2009; a039:1–11.
55. Um, I. H.; Oh, S. J.; Kwon D. S. Bull Korean Chem Soc 1996, 17, 802–807.
56. Pross, A. Adv Phys Org Chem 1977, 14, 69–126.
57. Kwon, D. S.; Park, J. Y.; Um, I. H. Bull Korean Chem Soc 1994, 15, 860–864.
58. Lee, I.; Lee, B. S.; Koh, H. J.; Chang, B. D. Bull Korean Chem Soc 1995, 16, 277–281.
59. Haake, P. J Am Chem Soc 1973, 95, 8088–8096.
60. Lee, I. Chem Soc Rev 1990, 19, 317–333.
61. Dubois, J.-E.; Ruasse, M.-F.; Argile, A. J Am Chem Soc 1984, 106, 4840–4845.
62. Ruff, F.; Farkas, Ö. J Org Chem 2006, 71, 3409–3416.
63. Ruff, F. Int Electron J Mol Des 2004, 3, 474–498.
64. Ruff, F. J Mol Struct (Theochem) 2003, 625, 111–120.
65. Ruff, F. J Mol Struct (Theochem) 2002, 617, 31–45.
66. Liu, L.; Guo, Q. X. Chem Rev 2001, 101, 673–695.
67. Linert, W.; Jameson, R. F. Chem Soc Rev 1989, 18, 477–505.
68. Linert, W. Chem Soc Rev 1994, 23, 429–438.
69. Exner, O. Chem Commun 2000, 1655–1656.
70. Hepler, L. G. Can J Chem 1971, 49, 2803–2807.
71. Exner, O. Collect Czech Chem Commun 1964, 29, 1094–1113.
72. Pal'm, V. A. Osnovy Kolichestvennoi Teorii Organicheskikh Reaktsii (Fundamentals of Quantitative Theory of Organic Reactions), 2nd ed.; Khimiya: Leningrad, Russia, 1977.
73. Leffler, J. E.; Grunwald, E. Rate and Equilibria of Organic Reactions as Treated by Statistical, Thermodynamic, and Extrathermodynamic Methods; Wiley: New York, 1963.
74. Lee, I. Adv Phys Org Chem 1992, 27, 57–117.
75. Kim, Y. S.; Choi, H.; Yang, K.; Park, J. K.; Koo, I. S. Bull Korean Chem Soc 2010, 31, 3279–3282.
76. Carniti, P.; Beltrame, P.; Cabiddu, S. J Chem Soc, Perkin Trans 2 1973, 1430–1433.
77. Sung, R. Y.; Choi, H.; Lee, J. P.; Park, J. K.; Yang, K.; Koo, I. S. Bull Korean Chem Soc 2009, 30, 1579–1582.
78. Williams, D. H.; Westwell, M. S. Chem Soc Rev 1998, 27, 57–63.
79. El-Bardan, A. A. J Phys Org Chem 1999, 12, 347–353.
80. More O'Ferrall, R. A. J Chem Soc B 1970, 274–277.

81. Jencks, W. P. Chem Rev 1972, 72, 705–718.
82. Castro, E. A.; Leandro, L.; Millan, P.; Santos, J. G. J Org Chem 1999, 64, 1953–1957.
83. Buncel, E.; Wilson, H.; Chuaqui, C. J Am Chem Soc 1982, 104, 4896–4900.
84. Arnett, E. M.; Reich, R. J Am Chem Soc 1980, 102, 5892–5902.
85. Koh, H. J.; Kang, S. J.; Kim Ch. J.; Lee, H. W.; Lee, I. Bull Korean Chem Soc 2003, 24, 925–930.
86. Oh, H. K.; Lee, j. Y.; Lee, H. W.; Lee, I. New J Chem 2002, 26, 473–476.
87. Oh, H. K.; Kim, S. K.; Lee, H. W.; Lee, I. J Chem Soc, Perkin Trans 2 2001, 1753–1757.
88. Oh, H. K.; Kim, S. K.; Cho, I. H.; Lee, H. W.; Lee, I. J Chem Soc, Perkin Trans 2 2000, 2306–2310.
89. Huisgen, R. Pure Appl Chem 1980, 52, 2283–2302.
90. Hine, J. Physical Organic Chemistry, 2nd ed.; McGraw-Hill: New York, 1962; p. 69.
91. Gould, E. S. Mechanism and Structure in Organic Chemistry; Holt, Rinehart and Winston: New York, 1959; p. 319.